New extraction of the $R_{e^+e^-}$ elastic scattering cross-section ratio based on a simplified phenomenological hard two-photon-exchange correction approach

I. A. Qattan,[1] A. Alsaad,[2] and A. A. Ahmad[2]

[1]Khalifa University of Science and Technology, Department of Physics, P.O. Box 127788, Abu Dhabi, United Arab Emirates
[2]Jordan University of Science and Technology, Department of Physical Sciences, P.O. Box 3030, Irbid 22110, Jordan

(Received 4 January 2021; revised 21 February 2021; accepted 29 April 2021; published 13 May 2021)

In this work, we present a prediction of the positron-proton and electron-proton elastic scattering cross-section ratio $R_{e^+e^-}$ based on a new phenomenological parametrization of the hard two-photon-exchange (TPE) corrections to electron-proton elastic scattering cross section σ_R. The TPE parametrization proposed in this work is rather simple, as it only requires the use of suitable global fits of both the Rosenbluth magnetic $\tilde{G}_M$, and the true magnetic G_M form factors, or alternatively, the electric form factors $\tilde{G}_E$ and G_E. We compare our results to recent extractions, and world's data on $R_{e^+e^-}$ with emphasis mainly on the kinematics range of the recent direct measurements from the CLAS, VEPP-3, and OLYMPUS experiments. With the proper choice of $\tilde{G}_M$ and G_M parametrizations, and while our results are in generally good agreement with $R_{e^+e^-}$ measurements taken at high ε points and for all Q^2 range, they agree remarkably well, within the error bands of the predictions, with $R_{e^+e^-}$ measurements taken at low-ε points for $Q^2 = 1.0$ and 1.5 $(\mathrm{GeV/c})^2$, where emphasis should be placed for evidence of hard TPE correction. Finally, we believe that the assumption that hard TPE corrections could account for the discrepancy on the proton's form factors ratio $\mu_p G_E/G_M$ is still an open question as more measurements of $R_{e^+e^-}$ are clearly needed for $Q^2 > 2.1$ $(\mathrm{GeV/c})^2$, in the region where the discrepancy is significant.

DOI: 10.1103/PhysRevC.103.055202

I. INTRODUCTION

Utilizing electron scattering, the proton's form factor (FF) ratio $\mu_p R_p = \mu_p G_E(Q^2)/G_M(Q^2)$ can be extracted using two main techniques: the Rosenbluth separation technique [1] and the polarization transfer (PT) or recoil polarization technique [2]. Here, $G_E(Q^2)$ and $G_M(Q^2)$ are the electric and magnetic FF of the proton, respectively, and μ_p is the proton's magnetic moment. These FFs are functions of the four-momentum transferred squared, Q^2, of the virtual photon, with longitudinal polarization parameter ε defined as $\varepsilon^{-1} = [1 + 2(1 + \tau)\tan^2(\frac{\theta_e}{2})]$, with $\tau = Q^2/4M_p^2$ being a kinematics factor, θ_e is the scattering angle of the electron, and M_p is the mass of the proton. In the Rosenbluth separation technique, the unpolarized electron-proton cross section is measured, and the reduced cross section σ_R in the one-photon-exchange approximation (OPE) or Born value is given by

$$\sigma_R(\varepsilon, Q^2) = [\tilde{G}_M(Q^2)]^2 + \frac{\varepsilon}{\tau}[\tilde{G}_E(Q^2)]^2. \tag{1}$$

In the PT technique, the spin-dependent cross section is measured, where the transverse P_t and longitudinal P_l polarization components of the recoil proton are measured simultaneously, and the ratio R_p in the OPE approximation [2–4] is determined as

$$R_p = \frac{G_E}{G_M} = -\frac{P_t}{P_l}\frac{(E+E')}{2M_p}\tan\left(\frac{\theta_e}{2}\right), \tag{2}$$

where E and E' are the initial and final energies of the incident electron, respectively.

The two techniques yield a significantly different value for the ratio $\mu_p R_p$ for $Q^2 > 1.0(\mathrm{GeV/c})^2$. They almost differ by a factor of 3 at high Q^2 [5–19] as the Rosenbluth separation method predicts scaling of the ratio $\mu_p R_p \approx 1$, while the PT method predicts a linearly decreasing $\mu_p R_p$ with increasing Q^2, and then flattening out for $Q^2 > 5.0$ $(\mathrm{GeV/c})^2$. Such a discrepancy on the ratio $\mu_p R_p$ was attributed to a missing higher order radiative corrections to σ_R, and in particular the inclusion of hard two-photon-exchange (TPE) correction diagrams [20–24]. This is accomplished by adding the contributions coming from the interference of the OPE and TPE amplitudes, or the real function $F(\varepsilon, Q^2)$, to the Born reduced cross section σ_{Born} or $\sigma_R(\varepsilon, Q^2) = \sigma_{\mathrm{Born}}(\varepsilon, Q^2) + F(\varepsilon, Q^2)$, and $G_{(E,M)}$ now represent the true FFs of the proton or

$$\sigma_R(\varepsilon, Q^2) = [G_M(Q^2)]^2 + \frac{\varepsilon}{\tau}[G_E(Q^2)]^2 + F(\varepsilon, Q^2). \tag{3}$$

Several studies have attempted to study the impact of TPE effects on electron-proton scattering observables theoretically [20,23–69], phenomenologically [17,70–95], and experimentally [11–13,96]. See Refs. [23,24,90,97] for detailed reviews. Experimentally, some studies focused mainly on measuring and/or constraining the TPE contributions to σ_R and the ratio $\mu_p R_p$ [12,13,16,17]. Other studies examined the ε dependence and nonlinearity of σ_R [70–72] and the ε dependence of the ratio $\mu_p R_p$ [11,96] to observe any possible deviation from the OPE prediction. However, the measured ratio showed essentially no ε dependence consistent with the OPE predictions. Phenomenologically, on the other hand, studies focused either on extracting the TPE contributions using combined elastic electron-proton cross section and polarization measurements [17,20,72,75,78–80,82,87–90,92], or extracting the TPE amplitudes by imposing some assumptions and constraints [74,76,83,84,86,90]. However, the most direct technique that can be used to measure TPE effect is by measuring the positron-proton to electron-proton cross sections ratio $R_{e^+e^-}(\varepsilon, Q^2)$ as the function $F(\varepsilon, Q^2)$ will change sign depending on the charge of the lepton involved. In addition, σ_R in the Born approximation is the measured elastic electron-proton cross section after applying radiative corrections which include photon radiation from the charged particle $\delta^{\pm}$ or simply $\sigma_R = \sigma_{\text{elastic}}(1 + \delta^{\pm})$, where $\delta^{\pm}$, $+(-)$ for positron(electron), includes vertex-type corrections or charge-even terms δ_{even}, and charge-odd terms δ_{odd} which change sign depending on the sign of the lepton involved, and include both hard-TPE ($\delta_{2\gamma}$) and soft-TPE (δ_{soft}) contributions or $\delta^{\pm} = \delta_{2\gamma} + \delta_{\text{soft}} + \delta_{\text{even}}$. Therefore, the measured ratio $R^{\text{meas}}_{e^+e^-}(\varepsilon, Q^2)$ is now defined as

$$R^{\text{meas}}_{e^+e^-}(\varepsilon, Q^2) = \frac{\sigma(e^+p \to e^+p)}{\sigma(e^-p \to e^-p)} = \frac{1 + \delta_{\text{even}} - \delta_{\text{odd}}}{1 + \delta_{\text{even}} + \delta_{\text{odd}}}, \tag{4}$$

and any deviation of $R^{\text{meas}}_{e^+e^-}$ from unity is a clear signature of δ_{odd} contributions to σ_R. Finally, after correcting $R^{\text{meas}}_{e^+e^-}$ for both δ_{even} and δ_{soft}, the ratio can be expressed as

$$R_{e^+e^-}(\varepsilon, Q^2) = \frac{1 - \delta_{2\gamma}}{1 + \delta_{2\gamma}} \approx 1 - 2\delta_{2\gamma}, \tag{5}$$

where $\delta_{2\gamma}$ is the fractional hard TPE correction to σ_R or $\delta_{2\gamma} = F(\varepsilon, Q^2)/\sigma_{\text{Born}}$, and any deviation of $R_{e^+e^-}(\varepsilon, Q^2)$ from unity is a clear signature of hard-TPE effect.

II. PHENOMENOLOGICAL TWO-PHOTON-EXCHANGE CONTRIBUTION

A. Linear hard TPE correction

In this section, we summarize several previous and recent TPE phenomenological studies and parametrizations used to extract the ratio $R_{e^+e^-}$. In particular, focus will be placed mainly on parametrizations which assumed linear TPE corrections to σ_R which are relevant to this work. See Refs. [78,79,83,84,86,90] for detailed review of other TPE phenomenological studies.

Based on the framework of Ref. [20], Borisyuk and Kobushkin [73] introduced the linear combination $\mathcal{G}_E = (\tilde{F}_1 - \tau\tilde{F}_2 + \frac{\nu}{4M_p^2}\tilde{F}_3)$ and $\mathcal{G}_M = (\tilde{F}_1 + \tilde{F}_2 + \varepsilon\frac{\nu}{4M_p^2}\tilde{F}_3)$ with $\tilde{F}_1$, $\tilde{F}_2$, and $\tilde{F}_3$ corresponding to $\tilde{G}_E$, $\tilde{G}_M$, and $\tilde{F}_3$, respectively. Expressing σ_R in terms of $\mathcal{G}_E$ and $\mathcal{G}_M$, and dropping terms of order α^2 yields

$$\sigma_R = \tau G_M^2 + \varepsilon G_E^2 + 2\varepsilon G_E\delta\mathcal{G}_E + 2\tau G_M\delta\mathcal{G}_M. \tag{6}$$

Because G_M is a factor of μ_p larger than G_E, the term $2\varepsilon G_E\delta\mathcal{G}_E$ is dropped in Eq. (6), and σ_R can now be written as

$$\sigma_R = \tau G_M^2 + \varepsilon G_E^2 + 2\tau G_M\delta\mathcal{G}_M. \tag{7}$$

Because of the linearity of the Rosenbluth plots based on the analyses of Refs. [71,72], $\mathcal{G}_M$ was parameterized linearly in ε as $\delta\mathcal{G}_M = [a(Q^2) + \varepsilon b(Q^2)]G_M(Q^2)$, where $a(Q^2)$ and $b(Q^2)$ are functions of Q^2. Since $a(Q^2)G_M^2 \ll \tau G_M^2$, σ_R can now be written as

$$\sigma_R = \tau G_M^2 + \varepsilon\big(G_E^2 + 2\tau b G_M^2\big), \tag{8}$$

with the proton's FFs ratio squared as extracted from the Rosenbluth separation method, written as

$$\left(\frac{\tilde{G}_E}{\tilde{G}_M}\right)^2 = R_{\text{LT}}^2 = \left(\frac{G_E}{G_M}\right)^2 + 2\tau b(Q^2), \tag{9}$$

and that extracted from the recoil-polarization method expressed as

$$\frac{G_E}{G_M} = R_p = \frac{\mathcal{G}_E}{\mathcal{G}_M}\left(1 - \frac{\varepsilon(1-\varepsilon)}{1+\varepsilon}Y_{2\gamma}\right). \tag{10}$$

Because the term $\frac{\varepsilon(1-\varepsilon)}{1+\varepsilon}Y_{2\gamma} \ll 1.0$, R_p was approximated as

$$R_p = \frac{\mathcal{G}_E}{\mathcal{G}_M} = \frac{G_E}{G_M}. \tag{11}$$

Solving for the TPE correction slope $b(Q^2)$ using Eqs. (9) and (11) yields

$$b(Q^2) = \frac{1}{2\tau}\big(R_{\text{LT}}^2 - R_p^2\big), \tag{12}$$

where R_{LT}^2 and R_p^2 were parametrized as a third-order polynomial in Q^2 as

$$R_{\text{LT}}^2 = \mu_p^{-2}[1.0736 - 0.1864Q^2 + 0.0358Q^4 + 0.0007Q^6] \tag{13}$$

and

$$R_p^2 = \mu_p^{-2}[1.1184 - 0.3256Q^2 + 0.0323Q^4 - 0.0014Q^6], \tag{14}$$

with the coefficient $b(Q^2)$ given by

$$b(Q^2) = \left[\frac{-0.0101}{Q^2} + 0.0314 + 0.0008Q^2 + 0.0005Q^4\right]. \tag{15}$$

In their later analysis [74], Borisyuk and Kobushkin applied the Regge limit where the TPE amplitude $\delta\mathcal{G}_M$ vanishes as $\varepsilon \to 1$, yielding

$$\delta\mathcal{G}_M/G_M = a(Q^2)(1-\varepsilon) \tag{16}$$

and

$$\sigma_R = G_M^2\big[\tau + \varepsilon R_p^2 + 2\tau a(Q^2)(1-\varepsilon)\big]. \tag{17}$$

The reduced cross section σ_R as expressed in Eq. (17) yields the following relations,

$$(\tilde{G}_E)^2 = G_E^2 - 2\tau a(Q^2)G_M^2, \tag{18a}$$

$$(\tilde{G}_M)^2 = [1 + 2a(Q^2)]G_M^2, \tag{18b}$$

with a cross-section slope or $R^2_{\rm LT}$:

$$R^2_{\rm LT} = \frac{R_p^2 - 2\tau a(Q^2)}{[1+2a(Q^2)]}, \tag{19}$$

and a TPE coefficient $a(Q^2)$:

$$a(Q^2) = \frac{R_p^2 - R^2_{\rm LT}}{2\left(\tau + R^2_{\rm LT}\right)}. \tag{20}$$

Based on the theoretical framework of Ref. [74], Qattan *et al.* [79] fitted the world data on σ_R for $Q^2 \geqslant 0.39$ (GeV/c)^2 to the form:

$$\sigma_R = G_M^2\left(1 + \frac{\varepsilon}{\tau}R_p^2\right) + 2a(Q^2)G_M^2(1-\varepsilon), \tag{21}$$

with G_M and the TPE coefficient $a(Q^2)$ being the parameters of the fit. The ratio R_p was constrained to its value as given by Gayou [7], and the TPE parameter $a(Q^2)$ was best parametrized as

$$a(Q^2) = [-0.0191\sqrt{Q^2} \pm 0.0014\sqrt{Q^2} \pm 0.003]. \tag{22}$$

In later analysis, and following the same procedure of Ref. [79], Qattan *et al.* [82] performed an improved extraction of the proton FFs and the TPE parameter $a(Q^2)$. They included the data sets used in Ref. [80] and additional low-Q^2 data from Refs. [17,98]. They also used their improved parametrization of $\mu_p R_p$ given by

$$\mu_p R_p = \frac{1}{1 + 0.1430Q^2 - 0.0086Q^4 + 0.0072Q^6}, \tag{23}$$

with an absolute uncertainty in the fit $\delta^2_{R_p}(Q^2) = \mu_p^{-2}\{(0.006)^2 + [0.015\ln(1+{\rm Q}^2)]^2\}$. The TPE parameter $a(Q^2)$ was best parametrized as $a(Q^2) = [0.016 - 0.030\sqrt{Q^2}]$, with Q^2 in (GeV/c)^2, and the ratio $R_{e^+e^-}$ was extracted using the form

$$R_{e^+e^-}(\varepsilon, Q^2) = \frac{1-\delta_{2\gamma}}{1+\delta_{2\gamma}} \approx 1 - \frac{4a(Q^2)(1-\varepsilon)}{\left(1 + \frac{\varepsilon}{\tau}R_p^2\right)}. \tag{24}$$

Recently [92], Schmidt extracted the ratio $R_{e^+e^-}$ assuming linear TPE correction to σ_R similar in form to that proposed in Ref. [74], Eq. (21):

$$\sigma_R = G_M^2 + \frac{\varepsilon}{\tau}G_E^2 - \delta(Q^2)(1-\varepsilon) = (\tilde{G}_M)^2 + \frac{\varepsilon}{\tau}(\tilde{G}_E)^2. \tag{25}$$

Note that $\delta = -2a(Q^2)G_M^2$ when compared to Eq. (21). Comparing similar terms on both sides of Eq. (25), we obtain

$$G_E^2 = (\tilde{G}_E)^2 - \tau\delta, \tag{26a}$$
$$G_M^2 = (\tilde{G}_M)^2 + \delta. \tag{26b}$$

Dividing both sides of Eq. (25), and solving for δ, we get

$$\delta(Q^2) = \frac{\mu_p^2(\tilde{G}_E)^2 - R_{FF}^2(\tilde{G}_M)^2}{R_{FF}^2 + \mu_p^2\tau}, \tag{27}$$

where $R_{FF} = \mu_p R_p$. The ratio $R_{e^+e^-}$ is then constructed as

$$R_{e^+e^-} = 1 - 2\delta_{2\gamma} = 1 + \frac{2\delta(1-\varepsilon)}{(\tilde{G}_E)^2 + \frac{\varepsilon}{\tau}(\tilde{G}_M)^2}, \tag{28}$$

using the recoil polarization ratio R_{FF} from Gayou [7], and the $\tilde{G}_{(E,M)}$ parametrizations from Bernauer [17], Arrington [22], and dipole parametrization $G_D(Q^2) = (1 + Q^2/[0.71({\rm GeV/c})^2])^{-2}$ for comparison.

B. New simple phenomenological hard TPE parametrization

In this section, we discuss the procedure used to extract the ratio $R_{e^+e^-}$ as a function of ε at fixed Q^2 value based on a new and simple phenomenological hard TPE parametrization. The procedure, together with the constraints and assumptions used, is outlined below:

(1) We relate the proton's FFs as obtained using the Rosenbluth separation (LT) method to the true FFs as

$$\tilde{G}_E = G_E + \delta G_E, \tag{29a}$$
$$\tilde{G}_M = G_M + \delta G_M, \tag{29b}$$

where $\delta G_{(E,M)}$ are small corrections and functions of Q^2 only.

(2) The reduced cross section σ_R, Eq. (1), can now be written as

$$\sigma_R = \tilde{G}_M^2 + \frac{\varepsilon}{\tau}\tilde{G}_E^2 = (G_M + \delta G_M)^2 + \frac{\varepsilon}{\tau}(G_E + \delta G_E)^2. \tag{30}$$

(3) Expanding and collecting similar terms, we have

$$\sigma_R = \left[G_M^2 + \frac{\varepsilon}{\tau}G_E^2\right] + (\delta G_M)^2 + 2G_M\delta G_M + \frac{\varepsilon}{\tau}[(\delta G_E)^2 + 2G_E\delta G_E], \tag{31}$$

where now the TPE correction $F(\varepsilon, Q^2) = (\delta G_M)^2 + 2G_M\delta G_M + \frac{\varepsilon}{\tau}[(\delta G_E)^2 + 2G_E\delta G_E]$.

(4) By imposing the Regge limit, where $F(\varepsilon = 1, Q^2) \to 0$, as $\varepsilon \to 1$, we get the following constraint:

$$(\delta G_M)^2 + 2G_M\delta G_M = -\frac{1}{\tau}[(\delta G_E)^2 + 2G_E\delta G_E]. \tag{32}$$

(5) Substituting the above constraint back in Eq. (31), we get

$$\sigma_R = \left[G_M^2 + \frac{\varepsilon}{\tau}G_E^2\right] + [(\delta G_M)^2 + 2G_M\delta G_M](1-\varepsilon). \tag{33}$$

(6) Completing the square by adding and subtracting G_M^2 in the second term of Eq. (33) above, and using $\tilde{G}_M = G_M + \delta G_M$, we get

$$\sigma_R = \left[G_M^2 + \frac{\varepsilon}{\tau}G_E^2\right] + \left[\tilde{G}_M^2 - G_M^2\right](1-\varepsilon) = \sigma_{\rm Born} + F(\varepsilon, Q^2), \tag{34}$$

or alternatively

$$\sigma_R = \left[G_M^2 + \frac{\varepsilon}{\tau}G_E^2\right] - \frac{1}{\tau}\left[\tilde{G}_E^2 - G_E^2\right](1-\varepsilon) = \sigma_{\text{Born}} + F(\varepsilon, Q^2). \tag{35}$$

(7) Finally, we define the fractional hard TPE correction to σ_R or $\delta_{2\gamma}$ as

$$\delta_{2\gamma} = \frac{F(\varepsilon, Q^2)}{\sigma_{\text{Born}}} = \frac{\left[\tilde{G}_M^2 - G_M^2\right](1-\varepsilon)}{\sigma_{\text{Born}}}, \tag{36}$$

and use it to construct the ratio $R_{e^+e^-}(\varepsilon, Q^2) = 1 - 2\delta_{2\gamma}$.

III. RESULTS AND DISCUSSION

In this section, we present our results of the ratio $R_{e^+e^-}$ as extracted using our new parametrization of the TPE contributions to electron-proton elastic scattering $F(\varepsilon, Q^2)$. Our TPE parametrization is rather simple as it only requires the use of suitable global fits of both the Rosenbluth magnetic FF $\tilde{G}_M$, and the true magnetic FF G_M, Eq. (34), along with their associated uncertainties, or alternatively, one can use the electric FFs $\tilde{G}_E$ and G_E as in Eq. (35). In addition, we compare our results to the recent extraction of Schmidt [92]. Our TPE parametrization is linear in ε, and vanishes as $\varepsilon \to 1$, similar to that used in Refs. [74,92]. However, the Q^2 dependence proposed in all three parametrizations is different. The Q^2 dependence proposed in Ref. [74] takes on the form $2a(Q^2)G_M^2$, Eq. (21), and in Ref. [92] it is given by $-\delta(Q^2)$, Eq. (27). In a typical analysis, the Q^2 dependence at a fixed Q^2 point is usually extracted by fitting the experimental electron-proton cross section to Eq. (3). Comparing the three different parametrizations, we see that $2a(Q^2)G_M^2 = -\delta(Q^2) = [(\tilde{G}_M/G_M)^2 - 1]G_M^2$.

It should be noted here that parametrizations where the TPE correction applied is linear or roughly linear function times G_M^2 will yield a ratio $R_{e^+e^-}$ that exhibits strong nonlinearity with ε at low ε and Q^2. With increasing Q^2, the ratio increases slowly, becomes roughly linear, and changes sign, above unity, where it behaves linearly with ε in good qualitative agreement with many previous phenomenological extractions, and TPE hadronic calculations [80,85,90]. In addition, the TPE contribution relative to G_M^2 is linear, but G_E^2 dominates σ_R at very low Q^2, except for $\varepsilon \to 0$, strongly suppressing TPE as a fractional contribution as one moves away from $\varepsilon = 0$.

In this analysis, we will use Eq. (34). While there are several unpolarized cross section global fits available for $\tilde{G}_M$, we will use, for consistency with the choice of parametrizations used in Ref. [92], the Arrington fit [22] and the Bernauer fit [17] (fit to the Mainz and World unpolarized cross-section measurements including Feshbach-Coulomb correction and using the Padé model), referred to throughout the text as "A" and "B," respectively, for comparison. The true magnetic FF G_M is usually extracted using parametrizations which account for hard TPE corrections. In this work, we first extract G_M using an unbiased approach which does not include any TPE corrections and then use G_M parametrization of Bernauer [17] (fit to the Mainz, World unpolarized cross section, and polarized ratio measurements including both Feshbach-Coulomb correction and phenomenological TPE model using the Padé model), referred to as "$B_{2\gamma}$" for comparison. For our extractions, we will use the recoil polarization ratio R_p and its associated uncertainty from Eq. (23). Therefore, our extraction of $R_{e^+e^-}$ involves four different versions where we use the following: (i) our TPE parametrization along with our G_M and Bernauer $\tilde{G}_M$ "This Work + B," (ii) our TPE parametrization along with our G_M and Arrington $\tilde{G}_M$ "This Work + A," (iii) our TPE parametrization along with Bernauer $\tilde{G}_M$ and Bernauer G_M "This Work + B + $B_{2\gamma}$," and (iv) our TPE parametrization along with Arrington $\tilde{G}_M$ and Bernauer G_M "This Work + A + $B_{2\gamma}$." In addition, we compare our ratio $R_{e^+e^-}$ to that extracted based on the parametrization of Schmidt, Eq. (28), where we use (i) Bernauer $\tilde{G}_{(E,M)}$ and Gayou R_{FF} "Schmidt + B" and (ii) Arrington $\tilde{G}_{(E,M)}$ and Gayou R_{FF} "Schmidt + A."

We first start with our G_M extraction and global fit. To extract G_M, we make use of the assumption that for $\varepsilon \to 1$, the TPE correction to σ_R vanishes (Regge limit) or $\sigma_R(\varepsilon = 1, Q^2) = [G_M^2 + G_E^2/\tau]$. In addition, because of the experimentally observed linearity of the Rosenbluth plots where σ_R data show a linear behavior in ε, suggesting the fit $\sigma_R = [c_1(Q^2) + \varepsilon c_2(Q^2)]$. Therefore, for a fixed Q^2 value, we linear fit σ_R to ε and extract the constants $c_1(Q^2)$ and $c_2(Q^2)$. Equating the two expressions for $\sigma_R(\varepsilon = 1, Q^2)$ yields

$$G_M^2 = \frac{c_1(Q^2) + c_2(Q^2)}{\left(1 + \frac{R_p^2}{\tau}\right)}, \tag{37}$$

where R_p is constrained to its value, along with its associated uncertainty, as given by Eq. (23).

World data on unpolarized σ_R used in analysis of Refs. [82,83], as well as new data from Refs. [12–15,17,98–101] were used, and fitted to extract G_M^2 based on Eq. (37) for a total of 142 Q^2 points up to $Q^2 = 5.2\ (\text{GeV}/c)^2$. For our G_M global fit, we fitted the extracted G_M/μ_p values to a functional form similar to that proposed by Kelly [102]:

$$\frac{G_M}{\mu_p} = \frac{1 + p_1 Q^2}{[1 + p_2 Q^2 + p_3 Q^4 + p_4 Q^6]}, \tag{38}$$

with $p_i (i = 1 - 4)$ being the parameters of the fit. The fitting procedure was based on the Levenberg-Marquardt nonlinear least squares fitting method with the reduced χ^2 ($\chi_\nu^2 = \chi^2/\nu$) defined as

$$\chi_\nu^2 = \frac{1}{\nu}\sum_{i=1}^{n_p=142}[(G_{M_i}/\mu_p)^{\text{meas.}} - (G_{M_i}/\mu_p)^{\text{comp.}}]^2/\sigma_i^2, \tag{39}$$

where $\nu = (n_{\text{p}} - n_{\text{parameters}})$ is the number of degrees of freedom. The χ_ν^2 value of the fit is reasonable and it equals $\chi_\nu^2 = 0.67$. The results of our G_M/μ_p fit are listed in Table I. In an attempt to improve the χ_ν^2 value obtained, we fitted to the functional form proposed by Arrington [22], which includes more fitting parameters, but the χ_ν^2 value did not improve significantly. We concluded that the obtained χ_ν^2 value is driven mainly by the tension between the different data sets and the

TABLE I. Fit parameters for $G_M(Q^2)/\mu_p$ using Eq. (38).

Quantity	p_1	p_2	p_3	p_4	χ^2_ν
G_M/μ_p	(0.2912 ± 0.0223)	(3.1970 ± 0.0256)	(2.3394 ± 0.07322)	(0.5881 ± 0.0414)	0.67

scatter of the data points, rather than a limitation of the fit function used.

Figure 1 shows the values of $G_M^p/\mu_p G_D$ extracted from this work (open dark-green squares), and our new $G_M^p/\mu_p G_D$ global fit (solid black line) along with its error bands (long-dashed black lines), as computed by using the covariance matrix of the fit. In addition, we also compare our results to the values as extracted based on hadronic calculations, labeled "AMT-Hadronic" [104] and "VAMZ" [103], and fits from previous phenomenological analyses labeled "Bernauer" [17], "Arrington-$Y_{2\gamma}$" [75], and "Puckett" [10]. At low Q^2, our results as well as our new fit are significantly above most previous fits. This clearly reflects the discrepancy between the Mainz data, which yield G_M values which are systematically 2–5% larger than previous world data [17]. At low Q^2 values, this corresponds to only a small difference in the cross section at large scattering angle. However, at larger Q^2 values of the Mainz experiment, this corresponds to a significant difference in the measured cross sections. Note that except for the Bernauer result, most of the previous phenomenological extractions of the FFs and TPE contributions were mainly focused on large Q^2 values, and so they did not always worry about how well the parametrizations of R_p reproduced low Q^2 data.

As a quick check on the validity of using Bernauer's G_M parametrization as an input for G_M in our parametrization, $[(\tilde{G}_M/G_M)^2 - 1]G_M^2(1-\varepsilon)$, and whether we are introducing an additional TPE correction on the top of the correction we are applying for the kinematics range considered in this work, we compared the Q^2 dependence term in our parametrization to that of Ref. [74] or $2a(Q^2)G_M^2 = [(\tilde{G}_M/G_M)^2 - 1]G_M^2$, and calculated the $a(Q^2)$ values using Bernauer's $\tilde{G}_M$ and G_M parametrizations.

Our $a(Q^2)$ values obtained ("This Work") and those predicted by Bernauer ("Bernauer") are shown in Fig. 2. In addition, we show curves representing $a(Q^2)$ as determined in previous analyses from Refs. [26] "BMT," [104] "AMT," [79] "QAA1," and [82] "QAA2." It should be noted here that Bernauer [17] applied a linear TPE correction of the form $\delta_{2\gamma} = -c_1 \ln(c_2 Q^2 + 1)(1-\varepsilon)$, on top of the low-$Q^2$

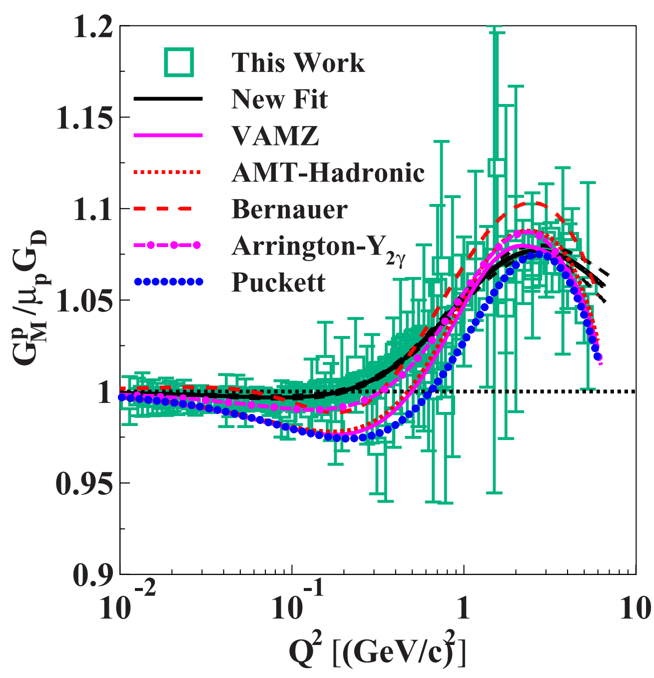

FIG. 1. $G_M^p/\mu_p G_D(Q^2)$ as obtained by using Eq. (37) and the parametrization of the ratio R_p from Eq. (23) (open dark-green squares). Our global fit of $G_M^p/\mu_p G_D(Q^2)$ (New Fit) is shown as a solid black line, along with its error bands (long-dashed black line). In addition, we compare the results to the extractions from several previous TPE calculations and phenomenological fits: VAMZ [103] (solid magenta line), AMT [104] (dotted red line), Bernauer [17] (long-dashed red line), Arrington $Y_{2\gamma}$ [75] (dash-dotted magenta line), and Puckett [10] (large-dotted blue line).

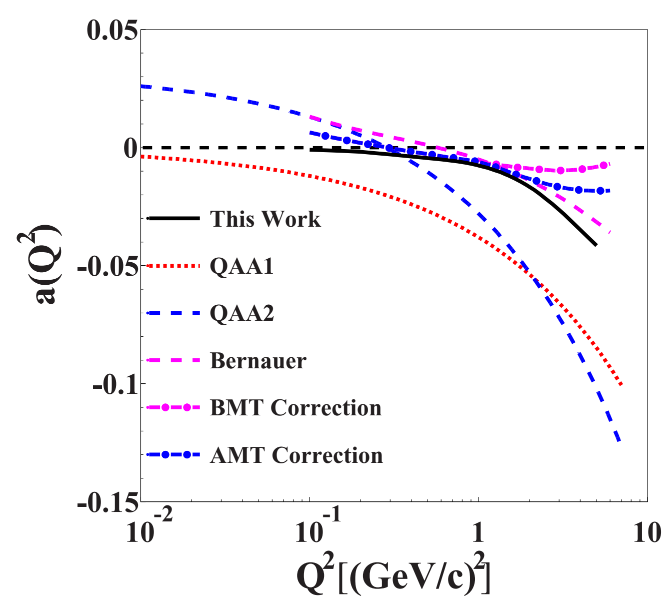

FIG. 2. The TPE coefficient $a(Q^2)$ as obtained using our parametrization assuming $\tilde{G}_M$ and G_M global fits from Ref. [17] "This Work" (solid black line). Also shown are curves representing $a(Q^2)$ as determined in previous analyses from Refs. [26] "BMT" (dash-dotted magenta line), [104] "AMT" (dash-dotted blue line), [79] "QAA1"(dotted red line), [82] "QAA2"(large-dashed blue line), and [17] "Bernauer" (large-dashed magenta line). Note that we do not show extractions of $a(Q^2)$ for the calculations or extraction of Ref. [17] at very low Q^2, as the ε dependence is quite different in our parametrization when the cross sections are dominated by the charge form factor. See text.

Feshbach-Coulomb correction $\delta_{\mathrm{Feshbach}}$. Here $c_{(1,2)}$ are constants. However, we do not show extractions of $a(Q^2)$ for the calculations or extraction of Ref. [17] at very low Q^2 as the ε dependence is quite different in our parametrization compared to that of Bernauer when the cross sections are dominated by the charge form factor.

Our values are in very good agreement with those of Bernauer, but with a small difference observed below $Q^2 = 0.60$ (GeV/c)^2, reaching a maximum value of 1.5% at $Q^2 = 0.10$(GeV/c)^2. This is clearly attributed to the additional low-Q^2 Feshbach-Coulomb correction applied by Bernauer. For the maximum difference at $Q^2 = 0.10$ (GeV/c)^2, this suggests a 1.5% (3.0% $\delta_{2\gamma}$) reduction in our $\delta_{2\gamma}(R_{e^+e^-})$ compared to that of Bernauer, which is very small. Therefore, any uncertainty introduced in our $R_{e^+e^-}$ as a result of using Bernauer G_M global fit is very small and can easily be accounted for within our quoted error bands on $R_{e^+e^-}$.

Figure 3 shows the ratio $R_{e^+e^-}$ as a function of ε extracted from this work, four different versions of the extraction, at the Q^2 values of the three new precise measurements by the CLAS collaboration [105], VEPP-3 Collaboration [106], and OLYMPUS Collaboration [107]. Note that for the experimental data, the measurement and the Q^2 value(s) are given in (GeV/c)^2. Also shown are the extractions based on the Schmidt parametrization [92]. In addition, we show the error bands on our "This Work + B + $B_{2\gamma}$" extraction, shown as a dotted magenta line, as computed by propagating the errors on $\delta_{2\gamma}$ in Eq. (36) using the uncertainties on $\tilde{G}_M$ and G_M from Ref. [17], and the uncertainty on the recoil polarization ratio δ_{R_p} (very negligible) from Eq. (23).

For $R_{e^+e^-}$ extraction based on the Schmidt parametrization [92], Eq. (28), the ratio $R_{e^+e^-}$ behaves linearly with ε, with small nonlinearity observed at low Q^2 points as expected. However, the "Schmidt + B" version predicts a ratio below unity, which changes sign (above unity) at $Q^2 = 0.2$ (GeV/c)^2, then starts to decrease slowly again, and changes sign (below unity again) with increasing Q^2. On the other hand, $R_{e^+e^-}$ as predicted using the "Schmidt + A" version is always above unity and increases with increasing Q^2.

For $R_{e^+e^-}$ extraction based on our parametrization, the ratio $R_{e^+e^-}$ is always above unity as predicted by all versions of the extraction, except for the "This Work + B" extraction for $Q^2 \gtrsim 1.0$ (GeV/c)^2. The ratio $R_{e^+e^-}$ is clearly sensitive to input $\tilde{G}_M$ and G_M parametrizations, with extractions using our G_M parametrization, "This Work + B" and "This Work + A," yielding larger ratio, with stronger nonlinearity at low ε for $Q^2 \lesssim 0.30$ (GeV/c)^2, than those obtained using Bernauer G_M, "This Work + B + $B_{2\gamma}$" and "This Work + A + $B_{2\gamma}$." In addition, and while most extractions predict a ratio that increases with increasing Q^2, the "This Work + B" extraction behaves differently as $R_{e^+e^-}$ increases up to $Q^2 = 0.2$ (GeV/c)^2, and then it starts to decrease with increasing Q^2 value where it changes sign (below unity) for $Q^2 \gtrsim 1.0$ (GeV/c)^2.

We now compare our extractions of the ratio $R_{e^+e^-}$ along with their associated error bands (calculated only for the "This Work + B + $B_{2\gamma}$" extraction, and shown as dotted magenta lines), to the world's data with focus primarily on the very recent direct and precise measurements from the

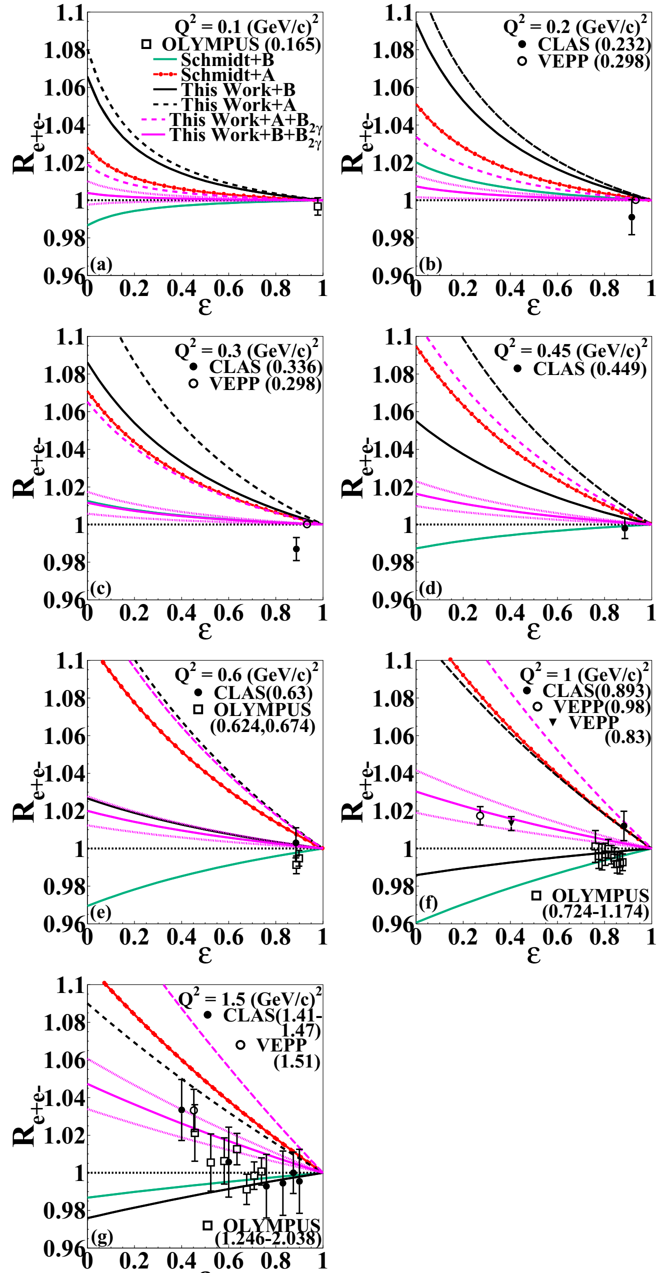

FIG. 3. The ratio $R_{e^+e^-}$ as a function of ε as extracted from this work (four different versions of the extraction) at the Q^2 values listed in the figure: "This Work + B" (solid black line), "This Work + A" (dashed black line), "This Work + B + $B_{2\gamma}$" (solid magenta line), and "This Work + A + $B_{2\gamma}$" (dashed magenta line). The error bands on $R_{e^+e^-}$ as extracted from "This Work + B + $B_{2\gamma}$" are shown as dotted magenta lines. Also shown is $R_{e^+e^-}$ as extracted based on the parametrization of Ref. [92]: "Schmidt + B" (solid dark-green line), and "Schmidt + A" (dash-dotted red line). See text for details. The data points are direct measurements of $R_{e^+e^-}$ from Refs. [105–107]. For the world data, the measurement and the Q^2 value(s) are given in (GeV/c)^2.

CLAS Collaboration [105], VEPP-3 Collaboration [106], and OLYMPUS Collaboration [107] at the Q^2 value listed in the figure. Note, however, that all three measurements measured the ratio $R_{e^+e^-}$ for $Q^2 < 2.1$ (GeV/c)^2 which is still below where the discrepancy on the ratio $\mu_p R_p$ is significant. Both CLAS and VEPP-3 data provided precise measurements of $R_{e^+e^-}$ at $Q^2 \approx 1.0$ and 1.5 (GeV/c)^2. The reported ratio $R_{e^+e^-}$ is larger than unity and exhibits clear ε dependence consistent with the FFs discrepancy at Q^2 values of 1.0-1.6 (GeV/c)^2. The data provided evidence for a sizable TPE contribution at larger Q^2 values, with clear deviation and change of sign from the exact calculations, high proton mass limit, at $Q^2 = 0$ [108], and finite-Q^2 calculations for a point-proton [23]. The $R_{e^+e^-}$ ratio as reported by the VEPP-3 Collaboration, however, exhibits a sharper Q^2 dependence, which tends to disappear when the results are compared to calculations that increase with Q^2 value. The OLYMPUS experiment measured the ratio $R_{e^+e^-}$ at Q^2 values of 0.165-2.038 (GeV/c)^2. The ratio is below unity at high ε, and then it changes sign (above unity) and starts to increase gradually reaching 2% at $\varepsilon = 0.46$. In conclusion, the results of these three recent measurements are in good agreement with each other within statistical and systematic uncertainties.

As we stated before, our parametrization is highly sensitive to the choice of input FFs parametrizations used. All extractions of the ratio $R_{e^+e^-}$ based on our parametrization, with its four different versions, and those of Schmidt, are in generally good agreement with existing data at large ε and for all the Q^2 points shown within the statistical and systematic uncertainties of these measurements, with the exception of the high ε measurement by CLAS at $Q^2 = 0.336$ (GeV/c)^2, and "some" of the high ε measurements by OLYMPUS taken in the range $0.6 \leqslant Q^2 \leqslant 2.038$ (GeV/c)^2, where these measurements are below the predicted $R_{e^+e^-}$ by some versions of the extractions. However, we believe that emphasis should only be placed on measurements taken at low-ε points as an evidence for hard TPE correction. Therefore, we see clearly that our TPE parametrization which uses Bernauer G_M and Bernauer $\tilde{G}_M$ as an input FFs or "This Work + B + $B_{2\gamma}$," agrees remarkably well, within the error bands of the extraction shown as dotted magenta lines, with direct measurements taken at low-ε points for $Q^2 = 1.0$ and 1.50 (GeV/c)^2.

Finally, the size of hard-TPE correction predicted in this work, and in several previous phenomenological extractions and TPE hadronic calculations is largely driven by the different assumptions used and constraints imposed in the analysis. Therefore, calculating the size of hard TPE correction in a model-independent way is very difficult, and the assumption that hard TPE corrections could account for the discrepancy on the ratio $\mu_p R_p$ is still an open question, as more measurements of the ratio $R_{e^+e^-}$ for $Q^2 > 2.1$ (GeV/c)^2 are clearly needed in the region where the discrepancy on the ratio $\mu_p R_p$ is significant.

IV. CONCLUSIONS

In conclusion, we presented a new extraction of the positron-proton and electron-proton elastic scattering cross-section ratio $R_{e^+e^-}$ based on a new parametrization of the TPE corrections to electron-proton elastic scattering cross section. Our TPE parametrization, Eq. (35), is rather simple as it only requires the use of suitable global fits of both the Rosenbluth magnetic FF $\tilde{G}_M$, and the true magnetic FF G_M, Eq. (34), along with their associated uncertainties. Alternatively, one can use the electric FFs $\tilde{G}_E$ and G_E as in Eq. (35). We compared our results to $R_{e^+e^-}$ extractions from Ref. [92], and world's data on $R_{e^+e^-}$ with emphasis mainly on the recent and precise direct measurements from Refs. [105–107].

In general, all extractions of the ratio $R_{e^+e^-}$ based on our parametrization, and that of Ref. [92], are in generally good agreement with existing world data at large ε and for all the Q^2 points shown, within the statistical and systematic uncertainties of these measurements, with the exception of the high-ε measurement by CLAS at $Q^2 = 0.336$ (GeV/c)^2 and some of the high-ε measurements by OLYMPUS taken in the range $0.6 \leqslant Q^2 \leqslant 2.038$ (GeV/c)^2, where these measurements are below the predicted $R_{e^+e^-}$ by some versions of the extractions. With emphasis placed only on measurements taken at low-ε points as an evidence for hard TPE correction, we find that our TPE parametrization which uses Bernauer G_M and $\tilde{G}_M$ [17] as an input FFs, "This Work + B + $B_{2\gamma}$," agrees remarkably well, within the error bands of the extraction, with direct measurements taken at low ε points for $Q^2 = 1.0$ and 1.50 (GeV/c)^2.

Finally, it should be emphasized here that calculating the size of hard TPE correction in a model-independent way is very difficult as the results are largely governed by the different assumptions used and constraints imposed in the analysis and calculations. Therefore, the assumption that hard TPE corrections could account for the discrepancy on the ratio $\mu_p R_p$ is still an open question. Clearly, more measurements of the ratio $R_{e^+e^-}$ for $Q^2 > 2.1$ (GeV/c)^2 are needed, in the region where the discrepancy on the FFs ratio $\mu_p R_p$ is significant.

ACKNOWLEDGMENT

The authors acknowledge the support provided by Khalifa University of Science and Technology.

[1] M. N. Rosenbluth, Phys. Rev. **79**, 615 (1950).
[2] N. Dombey, Rev. Mod. Phys. **41**, 236 (1969).
[3] A. I. Akhiezer and M. P. Rekalo, Fiz. Elem. Chast. Atom. Yadra **4**, 662 (1973) [Sov. J. Part. Nucl. **4**, 277 (1974)].
[4] R. G. Arnold, C. E. Carlson, and F. Gross, Phys. Rev. C **23**, 363 (1981).
[5] M. K. Jones *et al.*, Phys. Rev. Lett. **84**, 1398 (2000).
[6] O. Gayou *et al.*, Phys. Rev. C **64**, 038202 (2001).
[7] O. Gayou *et al.*, Phys. Rev. Lett. **88**, 092301 (2002).
[8] V. Punjabi *et al.*, Phys. Rev. C **71**, 055202 (2005).
[9] A. J. R. Puckett *et al.*, Phys. Rev. Lett. **104**, 242301 (2010).
[10] A. J. R. Puckett *et al.*, Phys. Rev. C **85**, 045203 (2012).
[11] A. J. R. Puckett *et al.*, Phys. Rev. C **96**, 055203 (2017); **98**, 019907(E) (2018).

[12] M. E. Christy *et al.*, Phys. Rev. C **70**, 015206 (2004).
[13] I. A. Qattan *et al.*, Phys. Rev. Lett. **94**, 142301 (2005).
[14] L. Andivahis *et al.*, Phys. Rev. D **50**, 5491 (1994).
[15] R. C. Walker *et al.*, Phys. Rev. D **49**, 5671 (1994).
[16] J. C. Bernauer *et al.* (A1 Collaboration), Phys. Rev. Lett. **105**, 242001 (2010).
[17] J. C. Bernauer *et al.* (A1 Collaboration), Phys. Rev. C **90**, 015206 (2014).
[18] J. Arrington, C. Roberts, and J. Zanotti, J. Phys. G **34**, S23 (2007).
[19] C. Perdrisat, V. Punjabi, and M. Vanderhaeghen, Prog. Part. Nucl. Phys. **59**, 694 (2007).
[20] P. A. M. Guichon and M. Vanderhaeghen, Phys. Rev. Lett. **91**, 142303 (2003).
[21] J. Arrington, Phys. Rev. C **68**, 034325 (2003).
[22] J. Arrington, Phys. Rev. C **69**, 022201(R) (2004).
[23] J. Arrington, P. Blunden, and W. Melnitchouk, Prog. Part. Nucl. Phys. **66**, 782 (2011).
[24] C. E. Carlson and M. Vanderhaeghen, Ann. Rev. Nucl. Part. Sci. **57**, 171 (2007).
[25] P. G. Blunden, W. Melnitchouk, and J. A. Tjon, Phys. Rev. Lett. **91**, 142304 (2003).
[26] P. G. Blunden, W. Melnitchouk, and J. A. Tjon, Phys. Rev. C **72**, 034612 (2005).
[27] S. Kondratyuk, P. G. Blunden, W. Melnitchouk, and J. A. Tjon, Phys. Rev. Lett. **95**, 172503 (2005).
[28] S. Kondratyuk and P. G. Blunden, Phys. Rev. C **75**, 038201 (2007).
[29] N. Kivel and M. Vanderhaeghen, Phys. Rev. Lett. **103**, 092004 (2009).
[30] N. Kivel and M. Vanderhaeghen, Phys. Rev. D **83**, 093005 (2011).
[31] N. Kivel and M. Vanderhaeghen, J. High Energy Physics 04 (2013) 029.
[32] O. Tomalak and M. Vanderhaeghen, Eur. Phys. J. A **51**, 24 (2015).
[33] Oleksandr Tomalak, Eur. Phys. J. A **55**, 64 (2019).
[34] I. T. Lorenz, U.-G. Meißner, H.-W. Hammer, and Y.-B. Dong, Phys. Rev. D **91**, 014023 (2015).
[35] Y. C. Chen, A. Afanasev, S. J. Brodsky, C. E. Carlson, and M. Vanderhaeghen, Phys. Rev. Lett. **93**, 122301 (2004).
[36] H. Okada and Y. Orikasa, Phys. Rev. D **93**, 013008 (2016).
[37] Y. M. Bystritskiy, E. A. Kuraev, and E. Tomasi-Gustafsson, Phys. Rev. C **75**, 015207 (2007).
[38] E. Tomasi-Gustafsson and G. I. Gakh, Phys. Rev. C **72**, 015209 (2005).
[39] D. Borisyuk and A. Kobushkin, Phys. Rev. C **74**, 065203 (2006).
[40] D. Borisyuk and A. Kobushkin, Phys. Rev. C **75**, 038202 (2007).
[41] D. Borisyuk and A. Kobushkin, Phys. Rev. C **78**, 025208 (2008).
[42] D. Borisyuk and A. Kobushkin, Phys. Rev. D **79**, 034001 (2009).
[43] D. Borisyuk and A. Kobushkin, Phys. Rev. C **86**, 055204 (2012).
[44] D. Borisyuk and A. Kobushkin, Phys. Rev. C **89**, 025204 (2014).
[45] D. Borisyuk and A. Kobushkin, Phys. Rev. C **92**, 035204 (2015).
[46] H. Q. Zhou, C. W. Kao, and S. N. Yang, Phys. Rev. Lett. **99**, 262001 (2007); **100**, 059903 (2008).
[47] H.-Q. Zhou, Chin. Phys. Lett. **26**, 061201 (2009).
[48] H.-Q. Zhou and S. N. Yang, Eur. Phys. J. A **51**, 105 (2015).
[49] K. M. Graczyk and C. Juszczak, J. Phys. G **42**, 034019 (2015).
[50] K. M. Graczyk, Phys. Rev. C **88**, 065205 (2013).
[51] K. M. Graczyk, Phys. Rev. C **84**, 034314 (2011).
[52] V. M. Braun, A. Lenz, and M. Wittmann, Phys. Rev. D **73**, 094019 (2006).
[53] P. G. Blunden and W. Melnitchouk, Phys. Rev. C **95**, 065209 (2017).
[54] O. Tomalak and M. Vanderhaeghen, Eur. Phys. J. C **78**, 514 (2018).
[55] O. Tomalak, B. Pasquini, and M. Vanderhaeghen, Phys. Rev. D **96**, 096001 (2017).
[56] O. Tomalak, Eur. Phys. J. C **77**, 517 (2017).
[57] O. Tomalak, B. Pasquini, and M. Vanderhaeghen, Phys. Rev. D **95**, 096001 (2017).
[58] C. E. Carlson, M. Gorchtein, and M. Vanderhaeghen, Phys. Rev. A **95**, 012506 (2017).
[59] O. Tomalak and M. Vanderhaeghen, Phys. Rev. D **93**, 013023 (2016).
[60] H.-Q. Zhou and S. N. Yang, Phys. Rev. C **96**, 055210 (2017).
[61] H.-Q. Zhou and S. N. Yang, JPS Conf. Proc. **13**, 020040 (2017).
[62] O. Koshchii and A. Afanasev, Phys. Rev. D **98**, 056007 (2018).
[63] R. J. Hill, Phys. Rev. D **95**, 013001 (2017).
[64] R. E. Gerasimov and V. S. Fadin, J. Phys. G **43**, 125003 (2016).
[65] C. E. Carlson, B. Pasquini, V. Pauk, and M. Vanderhaeghen, Phys. Rev. D **96**, 113010 (2017).
[66] O. Tomalak, Eur. Phys. J. C **77**, 858 (2017).
[67] O. Koshchii and A. Afanasev, Phys. Rev. D **96**, 016005 (2017).
[68] H.-Y. Cao and H.-Q. Zhou, arXiv:2005.08265 [nucl-th].
[69] J. Ahmad, P. G. Blunden, and W. Melnitchouk, Phys. Rev. C **102**, 045205 (2020).
[70] I. A. Qattan, Ph.D. thesis, Northwestern University, 2005, arXiv:nucl-ex/0610006.
[71] V. Tvaskis, J. Arrington, M. E. Christy, R. Ent, C. E. Keppel, Y. Liang, and G. Vittorini, Phys. Rev. C **73**, 025206 (2006).
[72] Y.-C. Chen, C.-W. Kao, and S.-N. Yang, Phys. Lett. B **652**, 269 (2007).
[73] D. Borisyuk and A. Kobushkin, Phys. Rev. C **76**, 022201(R) (2007).
[74] D. Borisyuk and A. Kobushkin, Phys. Rev. D **83**, 057501 (2011).
[75] J. Arrington, Phys. Rev. C **71**, 015202 (2005).
[76] J. Guttmann, N. Kivel, M. Meziane, and M. Vanderhaeghen, Eur. Phys. J. A **47**, 77 (2011).
[77] M. P. Rekalo and E. Tomasi-Gustafsson, Eur. Phys. J. A **22**, 331 (2004).
[78] I. A. Qattan and A. Alsaad, Phys. Rev. C **83**, 054307 (2011); **84**, 029905(E) (2011).
[79] I. A. Qattan, A. Alsaad, and J. Arrington, Phys. Rev. C **84**, 054317 (2011).
[80] I. A. Qattan and J. Arrington, Phys. Rev. C **86**, 065210 (2012).
[81] I. A. Qattan and J. Arrington, EPJ Web Conf. **66**, 06020 (2014).
[82] I. A. Qattan, J. Arrington, and A. Alsaad, Phys. Rev. C **91**, 065203 (2015).
[83] I. A. Qattan, Phys. Rev. C **95**, 055205 (2017).

[84] I. A. Qattan and J. Arrington, J. Phys. Conf. Ser. **869**, 012053 (2017).
[85] I. A. Qattan, Phys. Rev. C **95**, 065208 (2017).
[86] I. A. Qattan, D. Homouz, and M. K. Riahi, Phys. Rev. C **97**, 045201 (2018).
[87] V. V. Bytev and E. Tomasi-Gustafsson, Phys. Rev. C **99**, 025205 (2019).
[88] E. Tomasi-Gustafsson and S. Pacetti, Few Body Syst. **59**, 91 (2018).
[89] D. Borisyuk and A. Kobushkin, arXiv:1707.06164 [hep-ph].
[90] I. A. Qattan, S. P. Patole, and A. Alsaad, Phys. Rev. C **101**, 055202 (2020).
[91] I. A. Qattan, J. Phys. Conf. Ser. **1643**, 012192 (2020).
[92] A. Schmidt, J. Phys. G **47**, 055109 (2020).
[93] J. Arrington, Phys. Rev. C **69**, 032201(R) (2004).
[94] J. Arrington and I. Sick, Phys. Rev. C **70**, 028203 (2004).
[95] J. Arrington, J. Phys. G **40**, 115003 (2013).
[96] M. Meziane *et al.*, Phys. Rev. Lett. **106**, 132501 (2011).
[97] A. Afanasev, P. G. Blunden, D. Hasell, and B. A. Raue, Prog. Part. Nucl. Phys. **95**, 245 (2017).
[98] T. Janssens, R. Hofstadter, E. B. Hughes, and M. R. Yearian, Phys. Rev. **142**, 922 (1965).
[99] W. Bartel, F.-W. Büsser, W.-R. Dix, R. Felst, D. Harms, H. Krehbiel, J. McElroy, J. Meyer, and G. Weber, Nucl. Phys. B **58**, 429 (1973).
[100] J. Litt *et al.*, Phys. Lett. B **31**, 40 (1970).
[101] C. Berger, V. Burkert, G. Knop, B. Langenbeck, and K. Rith, Phys. Lett. B **35**, 87 (1971).
[102] J. J. Kelly, Phys. Rev. C **70**, 068202 (2004).
[103] S. Venkat, J. Arrington, G. A. Miller, and X. Zhan, Phys. Rev. C **83**, 015203 (2011).
[104] J. Arrington, W. Melnitchouk, and J. A. Tjon, Phys. Rev. C **76**, 035205 (2007).
[105] D. Adikaram *et al.* (CLAS Collaboration), Phys. Rev. Lett. **114**, 062003 (2015).
[106] I. A. Rachek *et al.* (VEPP-3 Collaboration), Phys. Rev. Lett. **114**, 062005 (2015).
[107] B. S. Henderson *et al.* (OLYMPUS Collaboration), Phys. Rev. Lett. **118**, 092501 (2017).
[108] W. A. McKinley and H. Feshbach, Phys. Rev. **74**, 1759 (1948).